AIAA JOURNAL
Vol. 46, No. 3, March 2008

Optimization of Aircraft Wings for Gust Loads: Interval Analysis-Based Approach

S. S. Rao* and Luna Majumder†
University of Miami, Coral Gables, Florida 33124-0624

DOI: 10.2514/1.33152

An interval-based approach is presented for the optimization of aircraft structures under dynamic loads. As a specific application, the design is considered by including the effect of uncertainty present in the atmospheric turbulence and other parameters on the dynamic response of the aircraft wing structure. The stresses induced during a gust encounter are considered as the primary behavior constraints. The optimization procedure is illustrated with two examples. One is a symmetric double-wedge airfoil and the other is a supersonic airplane wing. The design parameters of the aircraft wing are assumed to be uncertain which are described as interval quantities. Interval analysis is used in the computation of the objective and constraint functions of the problem. An interval-based nonlinear programming technique is developed for the optimum solution of the two aircraft wings considered. The present methodology is expected to be more realistic compared with the probabilistic and fuzzy approaches in situations where either the probability distribution functions or the preference information for the uncertain design parameters is not available.

Nomenclature

$[A]$, $[B]$, $[C]$, $[D]$	=	component matrices used in defining the aerodynamics matrix $[Q]$
A_{bi}	=	area of bar element
A_{si}	=	area of plate element
A_{wi}	=	area of web element
a	=	lift-curve slope
a_∞	=	freestream speed of sound
b	=	span of the wing
b_r	=	reference length
C	=	chord of the wing
c_0	=	chord at root of the wing
D	=	total drag
$F(y, t)$	=	applied load
$f_1(\boldsymbol{X})$	=	structural weight
$f_2(\boldsymbol{X})$	=	energy
$f_3(\boldsymbol{X})$	=	flutter velocity
K	=	stiffness matrix in flutter analysis
K_j	=	bending-moment factor
k_r	=	reduced frequency
l	=	semispan
l_{bi}	=	length of the ith bar element.
M_F	=	flutter Mach number
M_i	=	ith generalized mass
M_∞	=	flight Mach number
N	=	number of segments of airfoil
$P_i(t)$	=	ith generalized load
$p(y, t)$	=	intensity of load per unit length
$[Q]$	=	air force matrix used in flutter analysis
T	=	airfoil thickness
t	=	time parameter
U	=	flight velocity
u	=	vertical velocity of gust
V, V_∞	=	freestream velocity $= a_\infty M_\infty$
V_F	=	flutter velocity
$w_i(y)$	=	ith mode shape
x_j	=	jth design variable
ξ_i	=	ith generalized coordinate
$\boldsymbol{\xi}$	=	vector of modal participation coefficients
ρ	=	density of material
σ_g	=	maximum gust-induced stress
τ_f	=	duration of flight
$\varphi(t)$	=	Küssner function
ω	=	natural frequency
ω_F	=	flutter frequency
$\{1 - \phi(t)\}$	=	Wagner function

Received 29 June 2007; revision received 13 September 2007; accepted for publication 1 October 2007.

*Professor and Chairman, Department of Mechanical and Aerospace Engineering; srao@miami.edu. Associate Fellow AIAA.

†Graduate Student, Department of Mechanical and Aerospace Engineering.

Introduction

MANY uncertainties are associated with aerospace structural design in terms of loads, material properties, and geometric parameters. In certain situations, the uncertain parameters are to be modeled as interval-valued quantities. For example, the tolerances specified on the dimensions of an aircraft structure are directly connected with the capacity of the manufacturing process and the resulting cost of production. The dimensions, in this case, are to be represented as interval numbers. The wind (gust) loads acting on a wing may be known only in the form of a range, which implies that interval representation is suitable for describing the load. Similarly, if the available statistical data on material properties is limited, one can only describe the material properties as intervals ranging from their respective minimum and maximum limits. In these situations, compared to optimization with crisp and precise design parameters, optimization with imprecise parameters, based on interval representation, makes more sense. The optimum design of aircraft wings under gust loads is considered in this work using interval approach.

Two basic approaches are generally used for the structural design of an aircraft under gust encounter. One is a discrete gust approach, and the other is a random gust described by power-spectral techniques. In the discrete gust approach, the gust is assumed to be one-minus-cosine-type and uniform along the span of the wing. In the power-spectral technique, the vertical velocity due to gust is treated as a stochastic process for the computation of the gust-induced stresses. In the past, the design of aircraft for gusts has been based solely on the concept of a discrete gust by treating the airplane as a rigid body, but in later years, the fundamental wing bending deflection was also included in the dynamic-response calculations.

In recent years, airplane designs have usually incorporated both the single discrete gust (SDG) concept and the concept of a random gust, frequently represented by a statistical model. The discrete gust concept normally constitutes the core of the design approach, with the power-spectral portion used to include the dynamic-response effects more rationally. In the estimation of gust loads on airplanes, the maximum response to random gust is of main interest, especially for the purpose of structural design. After the derivation of the power spectrum of atmospheric turbulence from the available flight measurements, Press and Mazelsky made the application of power-spectral density (PSD) methods of analysis to gust-load problems [1]. The procedures used for the analysis of gust loads of the Lockheed L-1011 TriStar transport, which were based on the conventional time history analysis, were described by Stauffer and Hoblit [2]. Procedures for the optimum design of airplane wing structures under gust loads with deterministic and probabilistic stress analyses were presented by Rao [3]. Perry et al. [4] applied both the SDG and PSD methods to an airplane with linear aerodynamics to calculate the maximum gust loads. The SDG method is computationally more expensive than the PSD method because of the exhaustive search algorithm used. Tang and Dowell [5] developed a mathematical model and computational code in the time domain to calculate the nonlinear gust response of an aircraft with a high aspect ratio wing at low subsonic flow speeds.

Recently, it is recognized that reliability-based optimization (RBO) methods have the potential to generate designs that are more robust to uncertainty than conventional deterministic designs. An optimum design methodology is therefore needed at preliminary design stages that accounts for the inherent uncertainties present in the design parameters in a consistent manner; furthermore, this methodology should permit aerospace structural designers to continue using familiar design codes as much as possible. Yang and Nikolaidis [6] focused on gust design of wings, but use rather elementary structural and gust models to facilitate solving the system reliability problem associated with the stresses caused by gust loads. Their method does not take advantage of standard structural and aerodynamics tools, such as finite element analysis and double-lattice aerodynamics. Yang et al. [7] proposed a system-reliability-based design approach for light commuter aircraft wing structures under gust loads and have indicated that reliability-based optimization has the potential of improving dramatically the safety and efficiency of new designs.

The results obtained in the aforementioned works indicate that power-spectral methods are well suited for the calculation of loads in continuous rough air. But it is very difficult to determine the power-spectral-density function of atmospheric turbulence for a wide range of atmospheric conditions and the determination of the conditions under which normal distributions of the load time history apply. In addition, in all the previously cited works, the material properties were assumed to be deterministic. Because real-life conditions involve uncertain material properties, in addition to the uncertain vertical velocity due to the gust, it may not be realistic to perform the analysis and design computations using only crisp values. Probabilistic modeling technique is the traditional way of handling the uncertainty, but it cannot handle situations with incomplete or little information, or when that information is nonspecific, ambiguous, or conflicting. Hence, the uncertainties in structures need to be modeled on the basis of an alternative, nonprobabilistic, conceptual framework.

Many generalized models of uncertainty have been developed to treat different types of situations, including fuzzy sets and possibility theory, Dempster–Shafer theory of evidence, random sets, imprecise probabilities, and convex models. These generalized models of uncertainty have a variety of mathematical descriptions. However, they all are closely connected to interval analysis [8] in which the imprecision in an uncertain parameter is described by an interval. The finite element method with interval-valued parameters results in an interval finite element method (IFEM). Koyluoglu et al. [9] and Rao and Chen [10] have presented an optimization approach for the solution of equations associated with the IFEM solution. When the imprecise design parameters are expressed as interval numbers, the design equations can be converted to the form of interval expressions. The required computations can then be carried using the rules of interval arithmetic.

This paper presents an interval-based approach for the optimum design of wing structures for three different objectives subjected to stresses due to uncertain gust loads as the primary behavior constraint. The interval analysis and optimization methods use a truncation technique [11] to avoid wider intervals of response quantities. The optimization results are compared with those obtained using deterministic and probabilistic approaches in one of the examples.

Interval Analysis

When a system involves uncertainty in the form of linguistic parameters and vague data, the fuzzy approach can be used most conveniently for its description. Various efforts are being made to apply fuzzy set theory to solve structural optimization problems because there exists a vast amount of fuzzy information in both the objective and constraint functions during the optimum design of a practical structure [12]. If the system is fuzzy, it is possible to establish a connection between the interval method and fuzzy analysis using the concept of α cuts. The whole fuzzy set is divided into finite subsets by using discrete values of membership function. Each fuzzy subset represents the range of imprecision corresponding to a specified α value. Thus, an interval can be used to describe a fuzzy subset. By representing all the design parameters using the α-cuts approach, the interval expressions involved in the analysis and design of the system can be evaluated at different fuzzy levels or α values. In this paper, all the system parameters are treated as interval numbers as $A = [A - \Delta A, A + \Delta A]$ with A denoting the nominal value and ΔA the deviation from the mean. This involves the application of interval arithmetic to every step of calculations. Because it is not always possible to find detailed information on the uncertainty of a parameter, an interval statement can be conveniently used as a general indication of the imprecision that exists in an engineering design problem.

An interval number represents the range of uncertainty of design parameters. It can be denoted as $\tilde{x} = (\underline{x}, \bar{x}) \equiv (x^{(1)}, x^{(2)})$. Here, the lower- and upper-bound values are given by $\underline{x} = x^{(1)} = x_0 - \Delta x$ and $\bar{x} = x^{(2)} = x_0 + \Delta x$, where x_0 denotes the crisp or nominal value and Δx represents the tolerance on x. This represents the set $\{x | x^{(1)} \leq x \leq x^{(2)}\}$ of all real numbers between and including the endpoints x_1 and x_2. If the system is linear, the exact response can be computed using the combinatorial approach. If the response parameter is represented as $f(x_1, x_2, \ldots, x_n)$, where $x_1, x_2, \ldots, x_n$ denote the input interval parameters with

$$x_i = \left[x_i^{(1)}, \ x_i^{(2)}\right] \equiv [\underline{x}_i, \ \bar{x}_i]; \qquad i = 1, 2, \ldots, n \tag{1}$$

then all possible values of f are given by

$$\begin{gathered} f_r = f\left(x_1^{(i)}, \ x_2^{(j)}, \ldots, \ x_n^{(k)}\right); \qquad i = 1, 2 \\ j = 1, 2; \ldots; \qquad k = 1, 2; \qquad r = 1, 2, \ldots, 2^n \end{gathered} \tag{2}$$

where f_r denotes the value of the response parameter f at a particular combination of the end points of the intervals of $x_1, x_{2,\ldots,} x_n$. The response parameter can be denoted as an interval number as

$$f = [\underline{f}, \ \bar{f}] \equiv [\min_r f_r, \ \max_r f_r] \tag{3}$$

Although this method, known as the combinatorial method, appears to be simple, it requires 2^n analyses and becomes tedious and prohibitively expensive for most practical problems involving large numbers of interval parameters.

A real number x is equivalent to an interval $[x, x]$, which has zero width. The interval analysis can be conducted using interval arithmetic operations which are defined, for $X = [X_1, X_2]$ and $Y = [Y_1, Y_2]$, as

$$X + Y = [X_1 + Y_1, X_2 + Y_2] \tag{4}$$

$$X - Y = [X_1 - Y_2, X_2 - Y_1] \tag{5}$$

$$X \cdot Y = [\min(X_1 \cdot Y_1, X_1 \cdot Y_2, X_2 \cdot Y_1, X_2 \cdot Y_2), \max(X_1 \cdot Y_1, X_1 \cdot Y_2, X_2 \cdot Y_1, X_2 \cdot Y_2)] \tag{6}$$

$$X \div Y = [X_1, X_2] \cdot [1/Y_2, 1/Y_1] \tag{7}$$

Note that the division operation $X \div Y$ is not defined if $0 \in [Y_1, Y_2]$. We can see that interval addition and interval multiplication are both associative and commutative. While the subdistributive law and the inclusion monotonicity law hold true, interval computation can be extended to matrices, as well:

$$[A][B] = [C] = c_{ij}(p \times r) \tag{8}$$

With $[A] = a_{ij} = [\underline{a}_{ij}, \bar{a}_{ij}](p \times q)$, $[B] = b_{ij} = [\underline{b}_{ij}, \bar{b}_{ij}](q \times r)$, and the elements of the matrix $[C]$ are given by

$$c_{ij} = \sum_{k=1}^{q} a_{ik} b_{kj}; \qquad i = 1, 2, \ldots, p, \qquad i = 1, 2, \ldots, r \tag{9}$$

where the multiplication rule is to be used for each product $a_{ik}b_{kj}$. In general, each occurrence of a given variable in an interval computation is treated as a different variable. Thus, $X - X$ is computed as if it were $X - Y$ with Y numerically equal to, but independent of, X. This causes widening of computed intervals and makes it difficult to compute sharp numerical results of complicated expressions. This unwanted extra interval width is called the dependency problem. In complicated problems where there are large numbers of interval operations in each expression, a specific interval may appear several times in different terms of the same equation causing the width of the response parameters to be wider than the true width [11,13]. To limit the growth of intervals of response parameters for large amounts of uncertainty, an interval-truncation method (see the Appendix) can be used based on a comparison of the ranges of the input and output ranges of the parameters and the computed responses. The purpose of truncation is to make reasonable modifications to the output range before using it in the next interval operations.

Another inherent difficulty with interval arithmetic is that the range of the response parameters depends on the order or sequence in which the various interval input variables are used during the computations. To overcome this difficulty, the ranges of the response parameters obtained from interval arithmetic are checked and corrected (if necessary) with those given by the combinatorial approach at certain stages of optimization (particularly during the gradient computations).

Gust Analysis

By treating the wing similar to a beam, the differential equation for wing bending (neglecting structural damping) is given by

$$\frac{\partial^2}{\partial y^2} EI \frac{\partial^2 w}{\partial y^2} = m\ddot{w} + F \tag{10}$$

where the deflection of the wing w can be expressed according to the modal approach, as

$$w(y, t) = \sum_{i=0}^{n} w_i(y)\xi_i(t) \tag{11}$$

where $\xi_i(t)$ is the generalized coordinate and $w_i(y)$ is the ith mode shape. The equations of motion, in terms of the generalized coordinates, can be expressed as

$$M_i\ddot{\xi}_i(t) + \omega_i^2 M_i \xi_i(t) = P_i(t) \tag{12}$$

where $P_i(t)$ is the generalized force in the ith mode given by

$$P_i(t) = \int_{-\frac{b}{2}}^{\frac{b}{2}} F(y, t) w_i(y)\, \mathrm{d}y \tag{13}$$

where $F(y, t)$ denotes the applied force. When the airplane flies through a gust, the force F is composed of two parts [14]: the first one due to the vertical motion of the airplane L_v and the second one due to the gust L_g. On the basis of strip type of analysis, these two parts are defined as [15]

$$F = L_v + L_g = -\frac{a}{2}\rho c V \int_0^t \ddot{w}[1 - \phi(t - \tau)]\, \mathrm{d}\tau + \frac{a}{2}\rho c V \int_0^t \dot{u}\psi(t - \tau)\, \mathrm{d}\tau \tag{14}$$

where t is the time from the start of gust penetration, a is the lift-curve slope, ρ is the density of air, c is the chord of the wing, V is the forward velocity of flight, u is the vertical velocity of the gust, $\{1 - \phi(t)\}$ is the Wagner function, which denotes the growth of lift on a wing following a sudden change in angle of attack, and $\varphi(t)$ is the Küssner function, which denotes the growth of lift on a rigid wing penetrating a sharp-edge gust [15]. Because only two degrees of freedom (vertical motion and fundamental wing bending) are sufficient to accurately predict the response, by substituting Eq. (11) into Eq. (14), and the resulting equation for F into Eq. (12), the following two response equations result for $i = 0$ and 1, respectively:

$$\frac{2M_0}{a\rho VS}\ddot{\xi}_0 = -\int_0^t \left(\ddot{\xi}_0 + \frac{S_1}{S}\ddot{\xi}_1\right) \times \{1 - \phi(t - \tau)\}\, \mathrm{d}\tau + \int_0^t \dot{u}\psi(t - \tau)\, \mathrm{d}\tau \tag{15}$$

$$\frac{2M_1}{a\rho VS}\ddot{\xi}_1 + \frac{2\omega_1^2 M_1}{a\rho VS}\xi_1 = -\int_0^t \left(\frac{S_1}{S}\ddot{\xi}_0 + \frac{S_2}{S}\ddot{\xi}_1\right) \times \{1 - \phi(t - \tau)\}\, \mathrm{d}\tau + \frac{S_1}{S}\int_0^t \dot{u}\psi(t - \tau)\, \mathrm{d}\tau \tag{16}$$

where S, S_1, S_2, M_0, and M_1 can be defined in terms of the geometry and mode shapes of the wing. By introducing the nondimensional parameters s, σ, and z_1 as

$$s = 2V\frac{t}{c_0} \tag{17}$$

$$\sigma = 2V\frac{\tau}{c_0} \tag{18}$$

$$z_i = \frac{V}{Uc_0}\xi_i \qquad (i = 0, 1) \tag{19}$$

Eqs. (15) and (16) can be expressed, in an equivalent form, as

$$\mu_0\alpha = -2\int_0^s (\alpha + r_1\beta)\theta(s - \sigma)\, \mathrm{d}\sigma + f(s) \tag{20}$$

$$\frac{\mu_1}{r1}(\beta + \lambda^2 z_1) + 2\left(\frac{r_2}{r_1} - r_1\right) \times \int_0^s \beta\theta(s - \sigma)\, \mathrm{d}\sigma = \mu_0\alpha \tag{21}$$

where the expressions of μ_i, λ, r_i, α, β,θ, and f can be identified easily.

Stresses Induced in the Wing

Discrete Gust Concept

For the purpose of numerical evaluation, the interval between 0 and t is divided into m equal stations of interval (Fig. 1) ε so that $t_0 = s_0 = 0$ and $s_m = m\varepsilon$ or $t_m = m\varepsilon(c_0/2V)$ [from Eq. (19)]. Once the values of the generalized coordinates $\xi_0(t)$ or $[z_0(s)]$ and $\xi_1(t)$ or

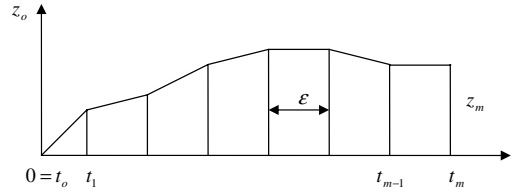

Fig. 1 Trapezoidal approximation for response calculation.

$[z_1(s)]$ are known at time stations $t = t_0 = 0$, $t_1 = \varepsilon(c_0/2V)$, $t_2 = 2\varepsilon(c_0/2V), \ldots, t_m = m\varepsilon(c_0/2V)$, the bending moment, and hence the bending stress that develops in the wing due to gust, may be found as follows. The total load acting on the wing at a section located at a distance y from the root of the wing is given by

$$p(y,t) = -m\ddot{w}(y,t) + F(y,t) \tag{22}$$

In view of Eqs. (17–19), Eq. (22) can be expressed as

$$\begin{aligned} p(\sigma,t) &= -m\frac{4UV}{c_0}[z_0'' + w_1(\sigma)z_1''] \\ &\quad - a\rho CUV\int_{\sigma=0}^{s}[z_0'' + w_1(\sigma)z_1''] \times \{1 - \phi(s-\sigma)\}\,\mathrm{d}\sigma \\ &\quad + \frac{a}{2}\rho CV\int_{\sigma=0}^{s} u\psi(s-\sigma)\,\mathrm{d}\sigma \end{aligned} \tag{23}$$

Thus, the bending moment induced at a distance of y_j from the root of the wing due to load $p(\sigma,t)$ is given by [15]

$$\begin{aligned} M_j(t) &= \int_{y=y_j}^{y=\frac{b}{2}} p(y,t)(y-y_j)\,\mathrm{d}y = -\frac{4UV}{co}\left[M_{m0}z_0'' + M_{m1}z_1''\right] \\ &\quad - a\rho UV\int_{\sigma=0}^{s}\left[Mcoz_o'' + Mc1z_1''\right]\{1-\phi(s-\sigma)\}d\sigma \\ &\quad + \frac{a}{2}\rho V\int_{\sigma=0}^{s}\left\{\int_{y_j}^{\frac{b}{2}} c(y-y_j)\,\mathrm{d}y\right\}u'\psi(s-\sigma)\,\mathrm{d}\sigma \end{aligned} \tag{24}$$

Division of Eq. (24) by the quantity $(a/2)\rho VUM_{c0}$ gives the bending-moment factor K_j at wing station y_j:

$$\begin{aligned} K_j &= \frac{M_j}{(a/2)\rho VUM_{c0}} = -\frac{8M_{m0}}{a\rho c_0 M_{c0}}\left(z_0'' + \frac{M_{m1}}{M_{m0}}z_1''\right) \\ &\quad - 2\int_{\sigma=0}^{s}\left(z_0'' + \frac{M_{c1}}{M_{c0}}z''\right)\{1-\phi(s-\sigma)\}\,\mathrm{d}\sigma \\ &\quad + \int_{\sigma=0}^{s}\frac{u'}{U}\psi(s-\sigma)\,\mathrm{d}\sigma \end{aligned} \tag{25}$$

The factor $(a/2)\rho VUM_{c0}$ may be regarded as the maximum aerodynamic bending moment that would be developed by the gust when the wing is considered rigid and restrained against vertical motion at the root. When the flow is quasi steady, the bending-moment factor K_j can be regarded as a response factor. A more convenient form for the bending-moment factor may be obtained by solving Eqs. (20) and (21), as

$$K_j(t) = dz_0'' + ez_1'' + h\lambda^2 z_1 \tag{26}$$

where d, e, and h are obtained from [15,16]. Once the bending-moment factor K_j is known at the time stations $t = t_0, t_1, \ldots, t_m$, the stresses induced at the wing section y_j at various instants of time can be found by knowing the sectional properties of the wing. Finally, the maximum stress induced in the wing due to gust can be determined as

$$\begin{aligned} &\sigma_g = \max[\text{stress induced at section } y_j \text{at time } t_i] \\ &i = 0, 1, 2, \ldots, m \text{ and out of all } j \end{aligned} \tag{27}$$

Power-Spectral Approach

The preceding approach works well for gusts which are isolated or which are of a continuous-sinusoidal type. But this approach is not very reliable because it is difficult to establish the time history of any long gust sequence. And so, to determine the effect of atmospheric turbulence on the dynamic response of an airplane, the atmospheric turbulence is modeled as a stationary random process. The power-spectral methods are used for finding the root mean square (rms) values of the stresses induced in the airplane wing structure. It is known that a simple relation exists for linear systems between the spectrum of the disturbance $\phi_\phi(\omega)$ and the spectrum of the system response to the disturbance $\phi_\psi(\omega)$, given by

$$\phi_\psi(\omega) = \phi_\phi(\omega)|H(\omega)|^2 \tag{28}$$

where $|H(\omega)|$ is the frequency response function. In Eq. (28), the turbulence is assumed to be one-dimensional; which means that at any instant of time, the vertical gust velocity is constant along the wing span or the scale of turbulence of the area under the correlation curve is large compared with the span of the wing. Figure 2 shows the PSD of vertical gust velocity. In this paper, the spectrum of the vertical gust velocity is taken as (Dryden's model [17])

$$\phi_\phi(\omega) = \frac{2L}{Vg}\left\{\frac{1 + \left(3L^2\omega^2/V_g^2\right)}{\left[1 + \left(L^2\omega^2/V_g^2\right)\right]^2}\right\}S_\phi^2 \tag{29}$$

where L is the scale of turbulence, ω is the frequency, and S_ϕ is the rms value of the gust velocity given by

$$S_\phi^2 = \int_{-\infty}^{\infty}\phi_\phi(\omega)\cdot\mathrm{d}\omega \tag{30}$$

The spectrum of the response can be used to determine the rms value of the response S_ψ as

$$S_\psi^2 = \int_{-\infty}^{\infty}\phi_\psi(\omega)\cdot\mathrm{d}\omega \tag{31}$$

For each frequency ω, the frequency response function $|H(\omega)|$, and hence the spectrum of the response, is computed by finding the stress response at a point in the airplane wing due to a unit sinusoidal gust. Because this sinusoidal gust can be treated as discrete, the deterministic gust analysis procedure described in the previous section can be used to find the transfer function $|H(\omega)|$. Thus, it becomes necessary to use the deterministic gust stress analysis a number of times in the probabilistic stress analysis.

The probabilistic approach cannot deliver reliable results with required precision without sufficient experimental data to validate the joint probability densities of the random variables or functions

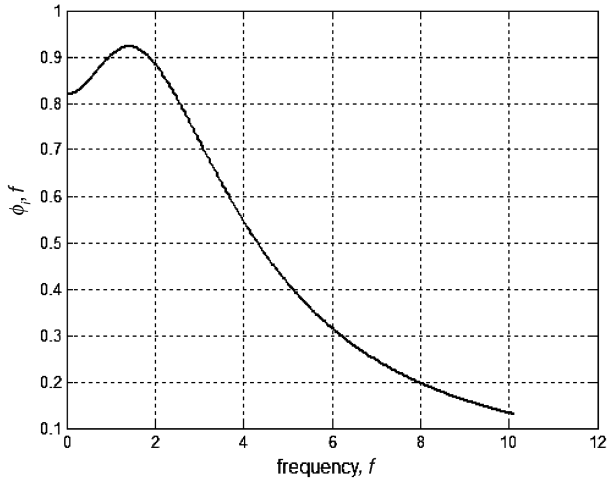

Fig. 2 Input power-spectral density for random continuous turbulence.

involved. Further, the determination of the power-spectral-density functions of atmospheric turbulence for a wide range of atmospheric conditions is difficult. In the interval parameters-based optimum design, on the other hand, only the known or expected ranges of the parameters are required. And so, if the parameters of a system are denoted by simple ranges, interval analysis methods can be used for the analysis of the system. In this approach, each system parameter is to be treated as an interval number as $(x - \Delta x, x + \Delta x)$, where x is the mean, deterministic, or nominal value of the parameter. And so, we need to apply interval arithmetic to every step of calculations. Because a specific interval may appear several times in different terms of the same equation, the order in which computations are carried will unnecessarily increase the interval ranges of the results [11,13]. Therefore, the dependence causes the loss of sharpness in the computed result. Thus, during programming, the truncation approach, which is based on a comparison between the ranges of the input parameters and the output responses of the system, is used.

Flutter Analysis

Equations for steady-state oscillations of the system in a state of neutral stability may be expressed [in generalized coordinates $\xi_i(t)$] as

$$[[K]_{s\times s} - \omega^2[M]_{s\times s} + [Q]_{s\times s}]\boldsymbol{\xi}_{s\times 1} = \mathbf{0}_{s\times 1} \tag{32}$$

where the $[K]$ and $[M]$ are the stiffness and mass matrices, respectively. The aerodynamic matrix, according to the piston theory, is given by

$$[Q^{(i)}] = 2\rho_\infty a_\infty V_\infty [A^{(i)}] + 2i\rho_\infty a_\infty w[B^{(i)}] + \rho_\infty(\gamma+1)V_\infty^2[C^{(i)}] + i\rho_\infty(\gamma+1)V_\infty\omega[D^{(i)}] \tag{33}$$

where the elements of the matrices $[A]$–$[D]$ are given by

$$[A^{(i)}] = \iint \boldsymbol{a}^T \frac{\partial \boldsymbol{a}}{\partial x}\,\mathrm{d}x\,\mathrm{d}y \tag{34}$$

$$[B^{(i)}] = \iint \boldsymbol{a}^T \boldsymbol{a}\,\mathrm{d}x\,\mathrm{d}y \tag{35}$$

$$[C^{(i)}] = \iint \frac{\partial Z}{\partial x}\boldsymbol{a}^T \frac{\partial \boldsymbol{a}}{\partial x}\,\mathrm{d}x\,\mathrm{d}y \tag{36}$$

$$[D^{(i)}] = \iint \frac{\partial Z}{\partial x}\boldsymbol{a}^T \boldsymbol{a}\,\mathrm{d}x\,\mathrm{d}y \tag{37}$$

The double integrals of Eqs. (34–37) are to be evaluated over the planform area of the ith element. The requirement for a nontrivial solution to Eq. (32) is that the determinant of the coefficient matrix of $\boldsymbol{\xi}$ must vanish. Thus, the flutter equation becomes

$$|[K] - \omega^2[M] + [Q]| = 0 \tag{38}$$

From Eq. (33), it can be seen that the elements of $[Q]$ are complex functions of the freestream velocity V_∞, oscillation frequency ω, density of air ρ_∞, and freestream speed of sound a_∞. For any given atmospheric conditions ρ_∞ and a_∞, Eq. (38) represents a complex, nonlinear, double eigenvalue problem because there are two unknowns, V_∞ and ω. Equation (38) can be written in a more convenient form as

$$\left|\frac{V}{a_\infty}\frac{1}{2\rho_\infty}[M_{ii}\{X(\omega_i/\omega_1)^2 - 1\}] + (b_r/k_r)^2\left([\mathrm{A}] + \frac{\gamma+1}{2}\frac{V}{a_\infty}[\mathrm{C}]\right) + i(b_r/k_r)\left([B] + \frac{\gamma+1}{2}\frac{V}{a_\infty}[D]\right)\right| = 0 \tag{39}$$

with $X = (\omega_1/\omega)^2$, $k_r = (b_r \cdot \omega/V) =$ reduced frequency, and $b_r =$ some reference length. The formulation of Eq. (39) is more convenient, compared with Eq. (38), to solve the flutter problem with Mach number (V/a_∞) and the reduced frequency (k_r) as the unknowns. In the present work, Eq. (39) is solved by a double iterative process, also known as the $V-g$ method. The lowest freestream velocity and the corresponding frequency obtained by solving Eq. (38) or Eq. (39) will be, respectively, the flutter velocity V_F and the flutter frequency ω_F.

Optimization Problem

Problem Statement

The optimization of two example wings is considered for illustration. The first example deals with the determination of the thickness T and chord length C of the hollow symmetric double-wedge airfoil shown in Fig. 3. The minimization of structural weight, minimization of and energy required, and maximization of flutter speed, while driving the airfoil through a specified flight condition, are treated as three different objectives. The maximum stress developed during gust σ_g is restricted to be less than a permissible value σ_g^u and bounds are placed on the design variables. Thus, the optimization problem becomes

Find $\boldsymbol{X} = \{x_1, x_2\} = \{T, C\}$ which minimizes $f_1(\boldsymbol{X})$, $f_2(\boldsymbol{X})$, and $f_3(\boldsymbol{X})$ (one at a time), subject to

$$\sigma_g(\boldsymbol{X}) \le \sigma_g^{(u)} \tag{40}$$

$$x_i^{(l)} \le x_i \le x_i^{(u)} \qquad i = 1, 2 \tag{41}$$

with the weight of the airfoil given by

$$f_1(\boldsymbol{X}) = \frac{1}{2}\rho l \rho_s x_1 x_2 \tag{42}$$

and the energy required by

$$f_2(\boldsymbol{X}) = D(\boldsymbol{X})VT_f \tag{43}$$

where ρ_s is the solidity ratio of the wing, V is the flight velocity, T_f is the duration of the flight, and D is the total drag which can be computed from the known flight conditions of the airfoil [18] as

$$D = D_p + D_f \tag{44}$$

where D_p and D_f represent the pressure and friction drags, respectively, with

$$D_p = \sum_{i=1}^{N_a} 2\gamma p_\infty M\left[\alpha_0 + \alpha_i + \left(\frac{T}{C}\right)^2\right]\frac{Cl}{N_a} \tag{45}$$

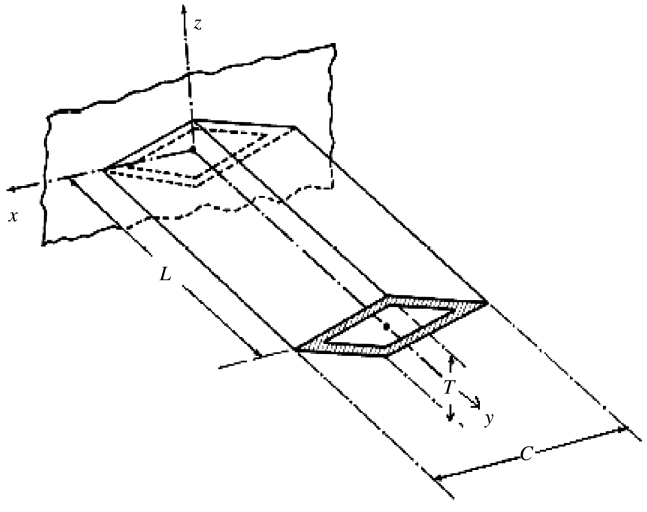

Fig. 3 Symmetric double-wedge airfoil (example 1).

and

$$D_f = \sum_{i=1}^{N_a}\left[\frac{2l}{N_a}\int_{-\frac{\xi}{2}}^{\frac{\xi}{2}} T'_f(x)\cos(\alpha_0+\alpha_i)\,\mathrm{d}x\right] \tag{46}$$

In Eqs. (45) and (46), p_∞ is the atmospheric pressure, γ the ratio of specific heat, M the flight Mach number, N_a the number of segments of the airfoil, and T'_f the shear stress, which are determined from the flight conditions [18]. The flutter Mach number is represented by $f_3(\boldsymbol{X})$.

In the second example (Fig. 4), both the structural weight of the supersonic wing and the energy required for a specific flight condition are minimized and the flutter velocity is maximized. The finite element method is used for structural idealization. The thicknesses of the skin, the thickness of the ribs and spars, and the cross-sectional areas of the pin-jointed bars are treated as design variables. The gust stress is constrained by an upper bound σ_g^u and the design variables are restricted to lie between specified limits. Thus, the optimization problem can be stated as

Find $\boldsymbol{X} = \{x_1, x_2, \ldots, x_6\}$ which minimizes $f_1(\boldsymbol{X})$, $f_2(\boldsymbol{X})$, and $f_3(\boldsymbol{X})$ separately, subject to

$$\sigma_g(X) \le \sigma_g^{(u)} \tag{47}$$

$$t_c^{(l)} \le t_{ci} \le t_c^{(u)} \tag{48}$$

$$t_w^{(l)} \le t_{\mathrm{wi}} \le t_w^{(u)} \tag{49}$$

$$A_b^{(l)} \le A_{\mathrm{bi}} \le A_b^{(u)} \tag{50}$$

with $f_1(\boldsymbol{X})$ = weight of the structure given by

$$f_1(\boldsymbol{X}) = \sum_{i=1}^{N_s}\rho t_{\mathrm{si}}A_{\mathrm{si}} + \sum_{i=1}^{N_w}\rho t_{\mathrm{wi}}A_{\mathrm{wi}} + \sum_{i=1}^{N_b}\rho l_{\mathrm{bi}}A_{\mathrm{bi}} \tag{51}$$

and $f_2(\boldsymbol{X})$ is given by Eq. (44) where D_p and D_f represent the pressure and friction drag with

$$D_p = 2M_\infty^2 P_\infty \iint_{\mathrm{SA}}\left[(\alpha_0 - w_x)^2 + \mathrm{d}_x^2 - \frac{1}{4}\gamma(1+\gamma)M_\infty^2(6\alpha_0\,\mathrm{d}_x w_x - 3\,\mathrm{d}_x w_x)\right]\mathrm{d}x\,\mathrm{d}y \tag{52}$$

and

$$D_f = \iint_{\mathrm{SA}}\left[\tau_{\mathrm{Fl}}\cos\left(\alpha_0 - \frac{\partial w}{\partial x} + \frac{\partial\,\mathrm{d}}{\partial x}\right) + \tau_{\mathrm{Fu}}\cos\left(\alpha_0 - \frac{\partial w}{\partial x} - \frac{\partial\,\mathrm{d}}{\partial x}\right)\right]\mathrm{d}x\,\mathrm{d}y \tag{53}$$

where τ_{Fl} and τ_{Fu} are the skin friction stress at the lower and upper surfaces of the wing, respectively, SA is the aerodynamic field, and $f_3(\boldsymbol{X})$ is the flutter Mach number.

Because all the system parameters, including the design variables and the objective functions, are treated as interval variables, we need to apply interval arithmetic to every step of the calculations. In addition, the truncation approach is used, which can give reasonable predictions for the solution even when the widths of their starting points or the interval ranges of other influencing parameters are quite large. In some computational steps, using interval arithmetic may not only seem to be redundant, but might lead to an invalid result which does not follow the physics of the equation. If these invalid operations are used in the computation, the final solution will be incorrect. To avoid such problems, a combinatorial approach is used

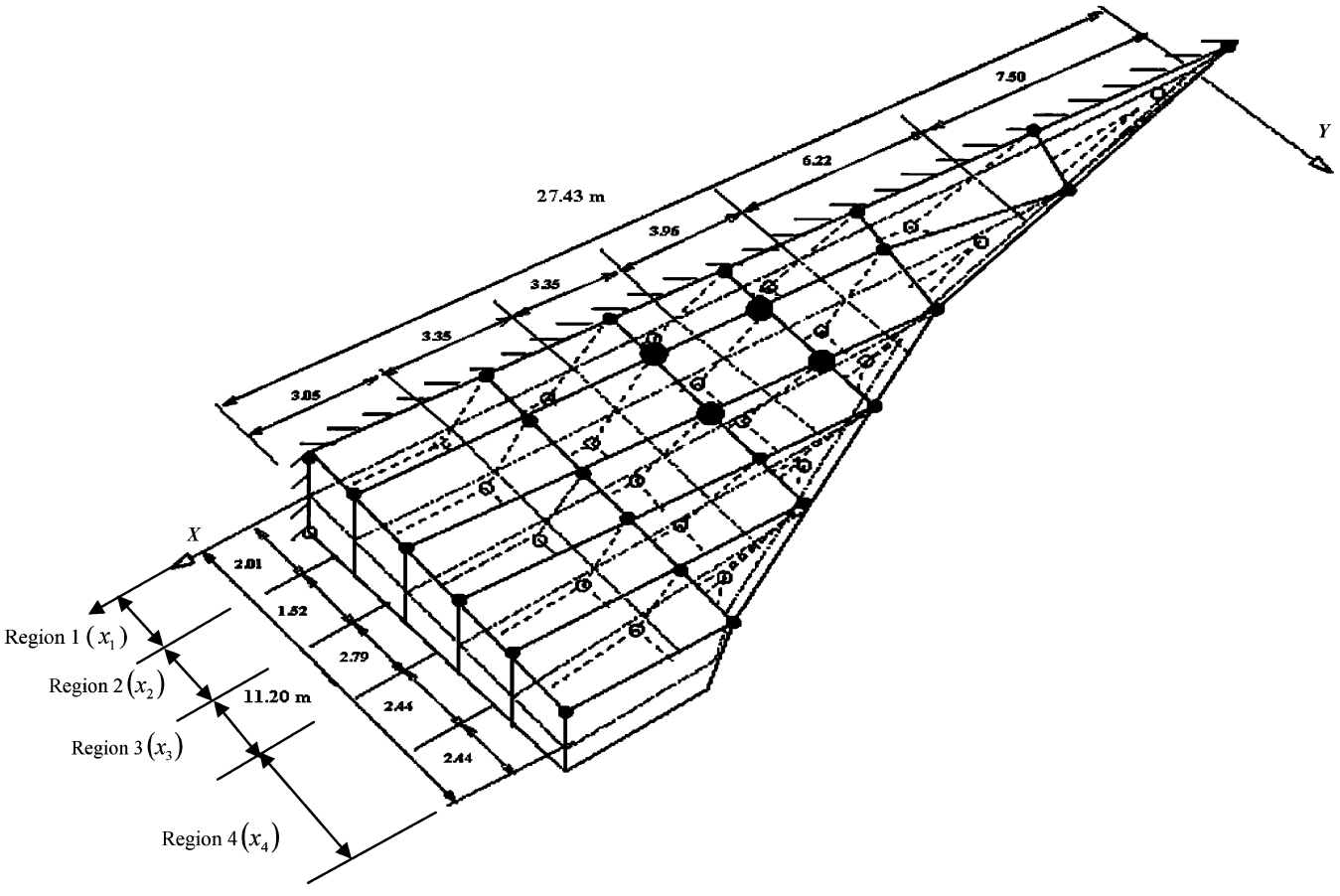

Fig. 4 Supersonic transport wing; finite element idealization (example 2).

instead of the interval operation to comply with the physical logic. Thus, it is necessary to understand the physical meaning of each equation before implementing the interval analysis.

Solution Procedure

The single-objective multivariable constrained optimization problems are solved using nonlinear programming techniques (penalty function approach and sequential quadratic programming) [19]. The cubic interpolation one-dimensional search method, Davidon–Fletcher–Powell (DFP) variable metric unconstrained minimization method, along with the interior penalty function method, is used in this (interval-based) work. In this approach, the optimization problem is converted to an unconstrained minimization problem by constructing a function of the form

$$\phi(\boldsymbol{X}, r_k) = f(\boldsymbol{X}) + r_k \sum_{j=1}^{m} G[g_j(\boldsymbol{X})] \tag{54}$$

where G is a function of the constraints defined as $G[g_j(\boldsymbol{X})] = -1/g_j(\boldsymbol{X})$. The minimization of the ϕ function is performed for a decreasing sequence of r_k. For the minimization of $\phi(\boldsymbol{X}, r_k)$, the starting feasible point $\boldsymbol{X}_0$ is found by a process of trial and error. Each subsequent stage used the solution of the previous stage as a starting point. For each r_k, the minimization of the ϕ function is terminated when the predicted percentage difference between the current and the optimal ϕ values is less than a small quantity ε. The value of ε used in the present work is 10^{-6} for example 1 and 0.0005 for example 2. A maximum of 10 cubic interpolations are allowed in each one-dimensional search problem. To test if any relative minima exist in the design space, two completely different starting points are used for the sequence of minimizations for one of the examples. The two sequences led to the same optimum design (except for a small difference which might have occurred due to numerical instability). Although, merely on the basis of two trial starting designs, it is hard to say that the minimum obtained is the global minimum, finding similar optimum designs by starting from two different initial designs is at least a pointer in that direction. It has been observed that some optimum design problems take a longer time to satisfy the prescribed convergence criterion after reaching very near to the optimum design. This phenomenon is very common if the objective function is highly distorted. In such cases, only a 1–2% reduction in the objective function can be achieved at the expense of 40–50% more computing time in the final stages. By using slightly relaxed convergence criterion, about 40% of computer time can thus be saved without losing more than 2% in the accuracy of optimum design. For comparison purposes, the corresponding deterministic and probabilistic optimization problems are solved using the MATLAB program based on sequential quadratic programming technique.

Numerical Results and Discussion

In the first example (Fig. 3) the airfoil is assumed to be made of titanium with Young's modulus 109.97 GPa, shear modulus 43.988 GPa, and weight density 4500 kg/m^3. The semispan is 9.0 m and the solidity ratio of the cross section is 0.075. The weights of the fuselage and the engines are 126.95 and 63.45 kg, respectively. The weight of the fuel is assumed to be distributed uniformly in the wing with a total weight of 105.38 kg. The duration of the flight is 1 h and the pull-up acceleration is $2g$. For structural analysis, the semispan of the airfoil is divided into five equal segments ($N = 5$), and the bending and torsional flexibility influence coefficients are used to find the natural frequencies. The airfoil is assumed to fly at a Mach number of 2.0 during the steady-state flight. The beam theory is used for the stress analysis of the airfoil. The thickness T and the chord length C, shown in Fig. 3, are the design variables. The discrete gust is assumed to be of cosine type with a maximum vertical velocity of 3.0 m/s, length of gust of 10 chords, forward velocity of flight 154.8384 m/s, and altitude 7618.049 m. For the power-spectral approach, the scale of turbulence is assumed as 762 m.

Table 1 Design data for example wing 2 [20]

Material properties	Material	Aluminum
	Young's modulus	68.948 GPa
	Poisson's ratio	0.333
	density	2768 kg/m^3
Details of the weight	planform area	136.99 m^2
	engines	5669 kg
	fuselage and payload	32,658.6 kg
	fuel	41,957.99 kg
	maximum takeoff mass	174,632.9 kg
Flight conditions data		
Altitude		7620.0 m
Pull-up acceleration		3.75 g
Flight Mach number		1.89
Pressure of air		37649.7 Pa
Density of air		0.5498 kg/m^3
Speed of sound		309.7 m/s
Gust analysis data		
Discrete gust, cosine type	maximum vertical velocity = 1.5233 m/s	
Length of gust = 5 chords	forward velocity of flight = 154.8384 m/s	
Altitude = 7618.05 m		
For spectrum approach	scale of turbulence = 7620 m	

The pertinent data for the second example wing (Fig. 4) are given in Table 1. For the interval analysis, each input parameter is represented as a range using the interval $(x - \Delta x, x + \Delta x)$ where x is the mean, deterministic, or nominal value of the parameter and Δx is the deviation from the mean value, taken as $0.05x$. For comparison purposes, a probabilistic analysis is performed by representing each parameter as a random variable following normal distribution, with known mean value x and standard deviation σ_x taken as one-third of Δx. By computing the mean value and standard deviations of outputs from the mean value and standard deviations of the input uncertain parameters, the constraints for probabilistic optimization can be approximated as

$$\bar{g} + 3S_g \leq g_{\text{limit}} \tag{55}$$

where $\bar{g}$ is the mean value, S_g is the standard deviation, and g_{limit} is the allowable limit for each constraint. The mean $\bar{g}$ and the standard deviation S_g are computed using the partial derivative rule, based on a first-order Taylor's series expansion of the function $g(\boldsymbol{Y})$ about the mean values of the unknown parameters y_i of the unknown parameter vector $\boldsymbol{Y}$.

In both the examples, the piston theory is used to calculate the aerodynamic drag. For probabilistic and interval analysis, each design variable is assumed to have a tolerance of $\pm 0.5\%$ (or $\pm 0.05x$) about the mean value. A computer program is developed for finding the optimum solutions. The optimum values of the weight, energy, and flutter Mach number for examples 1 and 2, corresponding to a fixed constraint value of $\alpha_g^{(u)}$, are shown in Tables 2–5. For comparison, the second wing problem is solved by considering the constraint and the objective functions with a probabilistic procedure. The results are reported in Table 4. For interval analysis, the problem is solved by treating all the design parameters as interval numbers. The optimum interval analysis-based designs, shown in Table 5, are found to be closer to the solutions obtained using the probabilistic analysis (Table 4).

Figure 5 shows the progress of objective functions with the three types of analyses. A sensitivity analysis is performed on the optimization results of example wing 2. Figure 6 shows the sensitivity of the gust-induced stress with the percent changes in the design variable values. For all the three types of analyses, it is found that the maximum gust stresses are most sensitive to variation of skin thickness near the root of the wing and least sensitive to variation of the thickness of spars and ribs (deterministic and probabilistic analyses) and area of stringers (interval analysis). These results are expected to be useful during the preliminary design of an airplane structure.

Table 2 Interval optimization results for double-wedge airfoil

	Initial design	Bounds		Optimum design, structural wt.	Optimum design, energy	Optimum design, flutter Mach no.
		Lower	Upper			
Design variables						
x_1, m	[0.4874 0.4879]	[0.16 0.22]	[2.46 3.00]	[0.3938 0.4803]	[0.3327 0.4900]	[0.5593 0.5708]
x_2, m	[5.7123 5.7177]	[0.60 0.76]	[5.99 7.83]	[5.6219 5.7421]	[6.9069 7.4481]	[4.5723 4.6424]
Behavior constraint						
Gust stress, σ_g, MPa	[20.5988 22.3223][a]	——	22.34	[18.1424 19.7705]	[17.015 18.1038]	[16.2415 17.1848]
Objective functions						
Structural wt., kg	[416.987 426.432]	——	——	[402.182 417.521]	[391.089 429.855]	[426.560 426.816]
Energy, GJ	[114.748 115.2942]	——	——	[73.981 127.60]	[58.211 83.3488]	[81.217 88.0030]
Flutter Mach no., negative value	[−7.4386 −7.4467]	——	——	[−7.7356 −3.3158]	[−7.2633 −4.2109]	[−9.9230 −9.2833]
No. of function evaluations	——	——	——	2532	666	151
No. of gradient evaluations	——	——	——	45	26	30

[a] active constraint

Table 3 Deterministic optimization results for wing (example 2)

	Initial design	Bounds		Optimum design, structural wt.	Optimum design, energy	Optimum design, flutter Mach no.
		Lower	Upper			
Design variables						
x_1, mm	2.539	1.0156	12.6950	1.3457	1.6078	5.2197
x_2, mm	2.539	1.0156	12.6950	1.7111	1.6179	3.048
x_3, mm	2.539	1.0156	12.6950	1.2954	1.5977	2.286
x_4, mm	2.539	1.0156	12.6950	1.4021	1.6205	1.81356
x_5, mm	6.3475	1.0156	16.5035	5.334	5.0673	6.25602
x_6, mm^2	161.29	25.7860	321.945	146.903	123.2900	246.3866
Behavior constraint						
Gust stress,σ_g, MPa	130.391	——	275.8	223.329	234.4921	216.7098
Objective functions						
Structural wt., kg	7338.727	——	——	3479.545	4510.454	10951.810
Energy, GJ	1823.716	——	——	1367.9529	1214.6059	1487.88
Flutter Mach no., negative value	−3.650	——	——	−6.9454	−4.0503	−6.9454
No. of function evaluations	——	——	——	441	232	173
No. of gradient evaluations	——	——	——	101	133	79

Conclusions

A methodology is presented for the interval analysis-based optimum design of airplane wing structures under gust loads. The optimum design procedure is demonstrated through the designs of a hollow symmetric double-wedge airfoil and a supersonic transport wing. Three different objectives, namely, the minimization of

Table 4 Probabilistic optimization results for wing (example 2)

	Initial design	Bounds		Optimum design, structural wt.	Optimum design, energy	Optimum design, flutter Mach no.
		Lower	Upper			
Design variables						
x_1, mm	2.539	1.0156	12.6950	3.6805	2.7051	11.143
x_2, mm	2.539	1.0156	12.6950	1.1735	1.3208	2.0942
x_3, mm	2.539	1.0156	12.6950	1.016	1.0185	1.7653
x_4, mm	2.539	1.0156	12.6950	1.2091	2.1082	1.4859
x_5, mm	6.3475	1.0156	16.5035	5.5804	18.996	9.8221
x_6, mm^2	161.29	25.7860	321.945	338.321	26.7096	104.451
Behavior constraint						
Gust stress,σ_g, MPa	130.474	——	304.759[a]	304.759*	234.6644	204.5747
Objective functions						
Structural wt., kg	7352.1364	——	——	3650.8636	4823.1818	10,210.4545
Energy, GJ	1835.296	——	——	1355.1187	1251.7809	1440.6803
Flutter Mach no., negative value	−3.452	——	——	−5.2974	−5.0093	−5.6723
No. of function evaluations	——	——	——	4672	5111	4942
No. of gradient evaluations	——	——	——	139	141	131

[a] active constraint

Table 5 Interval optimization results for wing (example 2)

	Initial design	Bounds		Optimum design, structural wt.	Optimum design, energy	Optimum design, flutter Mach no.
		Lower	Upper			
Design variables						
x_1, mm	[3.8034 3.8339]	1.0156	12.6950	[1.2590 1.3629]	[1.5926 1.6231]	[5.2121 5.2299]
x_2, mm	[3.8034 3.8339]	1.0156	12.6950	[1.6535 1.7958]	[1.5901 1.6231]	[3.0210 3.1471]
x_3, mm	[3.8034 3.8339]	1.0156	12.6950	[1.2853 1.3807]	[1.5901 1.6231]	[1.8186 2.3089]
x_4, mm	[3.8034 3.8339]	1.0156	12.6950	[1.3513 1.4453]	[1.5901 1.6231]	[1.6561 1.8339]
x_5, mm	[6.3424 6.3500]	1.0156	16.5035	[5.3264 5.4508]	[5.0546 5.0775]	[5.9462 6.7234]
x_6, mm^2	[161.0341 161.3550]	25.7860	321.9450	[144.451 147.8061]	[122.5158 128.9675]	[195.0963 296.1284]
Behavior constraint						
Gust stress,σ_g, MPa	[126.5371 131.8530]	——	275.8	[223.094 236.236]	[202.8710 243.5038]	[196.0801 227.7832]
Objective functions						
Structural wt., kg	[7302.318 7375.445]	——	——	[3386.136 3513.045]	[3644.591 3699.818]	[8959.091 10226.818]
Energy, GJ	[1823.568 1823.9373]	——	——	[1322.4430 1413.905]	[1214.0896 1214.753]	[1401.5963 1559.8978]
Flutter Mach no., negative value	[−3.6608 −3.6378]	——	——	[−5.2182 −3.5503]	[−6.2997 −5.9970]	[−7.8240 −6.1403]
No. of function evaluations	——	——	——	347	307	229
No. of gradient evaluations	——	——	——	93	151	87

structural weight, minimization of energy, and maximization of flutter Mach number during a specified flight condition, are considered in the problem formulation. The results obtained with the interval analysis-based approach are found to be in good agreement with the one obtained using a deterministic analysis for comparable data. Because of the random natures of the forward velocity and vertical velocity of gust, a probabilistic approach is also used and the resulting optimization results are compared with those obtained using deterministic and interval analyses. The optimization results obtained with interval analysis are found to be in good agreement with those obtained with the probabilistic approach. Because the actual value of the gust loads or their probability distributions cannot be predicted precisely, the interval analysis is expected to be more useful in certain cases and can be used for the optimum design of airplane wing structures.

Appendix: Truncation Procedure

Let two interval numbers $a = [\underline{a},\ \bar{a}]$ and $b = [\underline{b},\ \bar{b}]$ be used to compute $c = [\underline{c},\ \bar{c}]$. If we use the central values of the variables $a_0 = (\underline{a} + \bar{a})/2$ and $b_0 = (\underline{b} + \bar{b})/2$ to do the same (crisp) calculation, we get the output c_0. Then we use c_0 to judge the necessity of applying truncation. Let $\varepsilon = 10^{-5}$ represent a very small number. Then we try to obtain the refined results as $c \approx [\underline{d},\ \bar{d}]$. If c_0 is close to zero, no truncation needs to be used:

$$\underline{d} = \underline{c}; \qquad \bar{d} = \bar{c}; \quad \text{if } c_0 \le \varepsilon \tag{A1}$$

Otherwise, the truncation method is implemented as follows:

1) Find the relative deviation Δ of the interval range $(\bar{c} - \underline{c})$ as

$$\Delta_1 = \left|\frac{c_0 - \underline{c}}{c_0}\right|; \qquad \Delta_2 = \left|\frac{\bar{c} - c_0}{c_0}\right|; \qquad \Delta = \Delta_1 + \Delta_2 = \bar{c} - \underline{c} \tag{A2}$$

2_ Because the deviation Δ should be larger or equal to the exact deviation, we specify the maximum permissible range of $(\bar{c} - \underline{c})$ to be equal to $2t$. Time t can be selected to be equal to the maximum of the relative deviations of the input variables a and b from their respective central values:

$$t = \max\left(\left|\frac{\bar{a} - \underline{a}}{a_0}\right|, \left|\frac{\bar{b} - \underline{b}}{b_0}\right|\right) \tag{A3}$$

3 Use t to compare the deviations, and the range of c is truncated according to the following scheme:

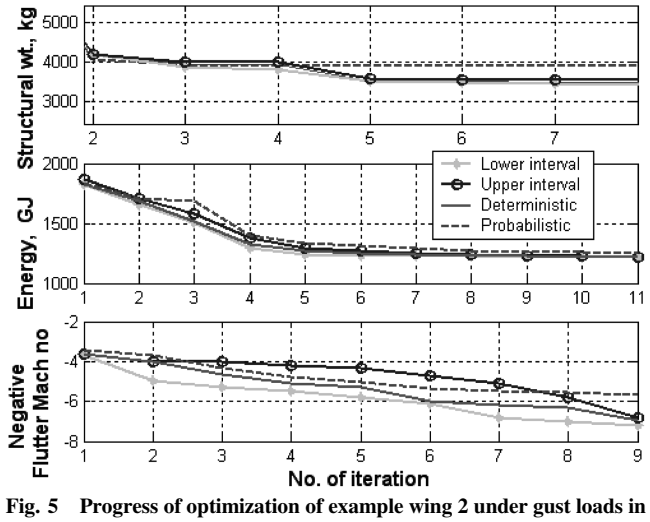

Fig. 5 Progress of optimization of example wing 2 under gust loads in deterministic, probabilistic, interval analyses.

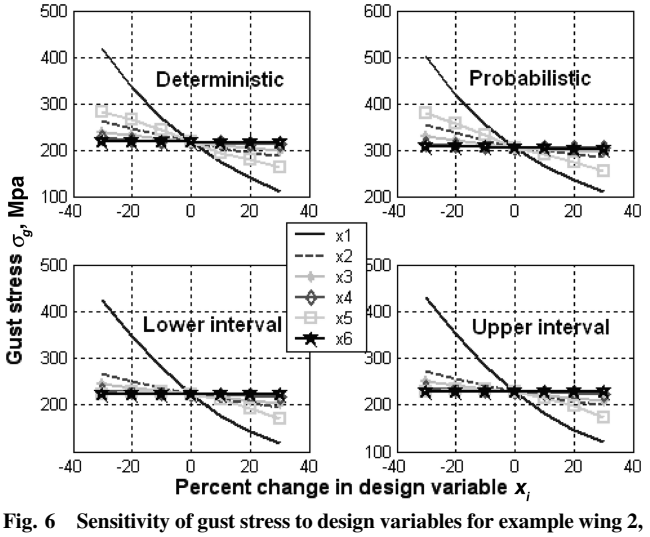

Fig. 6 Sensitivity of gust stress to design variables for example wing 2, with deterministic, probabilistic, and interval analyses (objective, structural weight).

$$\underline{d} = \underline{c}; \qquad \bar{d} = \bar{c}; \quad \text{if } \Delta_1 \le t \quad \text{and} \quad \Delta_2 \le t$$
$$\underline{d} = c_0 + t(\underline{c} - c_0); \qquad \underline{d} = \underline{c}; \quad \text{if } \Delta_1 > t \quad \text{and} \quad \Delta_2 \le t$$
$$\underline{d} = \underline{c}; \qquad \bar{d} = c_0 + t(\bar{c} - c_0); \quad \text{if } \Delta_1 \le t \quad \text{and} \quad \Delta_2 > t$$
$$\underline{d} = c_0 + t(\underline{c} - c_0)$$
$$\bar{d} = c_0 + t(\bar{c} - c_0); \quad \text{if } \Delta_1 > t \quad \text{and} \quad \Delta_2 > t \tag{A4}$$

In numerical experiments, compared with the combinatorial method, the truncation method is found to be fast and fairly accurate [11].

References

[1] Press, H., and Mazelsky, B., "Study of the Application of Power-Spectral Methods of Generalized Harmonic Analysis to Gust Loads on Airplanes," NACA, Rept. 2853, 1953.

[2] Stauffer, W. A., and Hoblit, F. M., "Dynamic Gust, Landing and Taxi Loads Determination in the Design of the L-1011," *Journal of Aircraft*, Vol. 10, No. 5, 1973, pp. 459–467.

[3] Rao, S. S., "Optimization of Airplane Wing Structures Under Gust Loads," *Computers and Structures*, Vol. 21, No. 4, 1985, pp. 741–749. doi:10.1016/0045-7949(85)90150-6

[4] Perry, B., III, Pototzky, A. S., and Wood, J. A., "NASA Investigation of a Claimed Overlap Between Two Gust Response Analysis Method," *Journal of Aircraft*, Vol. 27, No. 7, 1990, pp. 605–611.

[5] Tang, D., and Dowell, E. H., "Experimental and Theoretical Study of Gust Response for High-Aspect-Ratio Wing," *AIAA Journal*, Vol. 40, No. 3, 2002, pp. 419–429.

[6] Yang, J-S., and Nikolaidis, E., "Design of Aircraft Wings Subjected to Gust Loads: A Safety Index Based Approach," *AIAA Journal*, Vol. 29, No. 5, 1991, pp. 804–812.

[7] Yang, J-S., Nikolaidis, E., and Haftka, R. T., "Design of Aircraft Wings Subjected to Gust Loads: A System Reliability Approach," *Computers and Structures*, Vol. 36, No. 6, 1990, pp. 1057–1066. doi:10.1016/0045-7949(90)90213-L

[8] Moore, R. E., *Interval Analysis*, Prentice–Hall, Englewood Cliffs, NJ, 1966.

[9] Koyluoglu, U., Cakmak, S., Ahmet, N., and Soren, R. K., "Interval Algebra to Deal with Pattern Loading and Structural Uncertainty," *Journal of Engineering Mechanics*, Vol. 121, No. 11, Nov. 1995, pp. 1149–1157. doi:10.1061/(ASCE)0733-9399(1995)121:11(1149)

[10] Rao, S. S., and Chen, L., "Numerical Solution of Fuzzy Linear Equations in Engineering Analysis," *International Journal for Numerical Methods in Engineering*, Vol. 43, No. 3, 1998, pp. 391–408. doi:10.1002/(SICI)1097-0207(19981015)43:3<391::AID-NME417>3.0.CO;2-J

[11] Rao, S. S., and Berke, L., "Analysis of Uncertain Structural Systems Using Interval Analysis," *AIAA Journal*, Vol. 35, No. 4, 1997, pp. 727–735.

[12] Zadeh, L. A., "Fuzzy Sets," *Information and Control*, Vol. 8, No. 3, 1965, pp. 338–353. doi:10.1016/S0019-9958(65)90241-X

[13] Hnsen, E., and Walster Soren, G. W., *Global Optimization Using Interval Analysis*, 2nd ed., Marcel Dekker, New York, 2004.

[14] Hoblit, F. M., *Gust Loads on Aircraft: Concepts and Applications*, AIAA Education Series, AIAA, New York, 1988.

[15] Houbolt, J. C., and Kordes, E. E., "Structural Response to Discrete and Continuous Gusts of an Airplane Having Wing Bending Flexibility and a Correlation of Calculated and Flight Results," NACA, Rept. 1181, 1954.

[16] Houbolt, J. C., "Recurrence Matrix Solution for the Dynamic Response of Aircraft in Gusts," NACA, Rept. 1010, 1951.

[17] Houbolt, J. C., Steiner, R., and Pratt, K. G., "Dynamic Response of Airplanes to Atmospheric Turbulence including Flight Data on Input and Response," NASA TR R-199, 1964.

[18] Schmit, L. A., and Thronton, W. A., "Synthesis of an Airfoil at Supersonic Mach Number," NASA, Rept. CR-144, 1965.

[19] Rao, S. S., *Engineering Optimization: Theory and Practice*, 3rd ed., Wiley, New York, 1996.

[20] *Aviation Week & Space Technology*, McGraw–Hill, New York, 8 Feb. 1971, p. 42.

E. Livne
Associate Editor